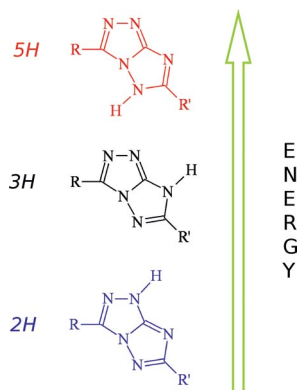


Triazole Tautomerism

[1,2,4]Triazolo[3,2-*c*][1,2,4]triazole has three tautomers: *2H*, *3H* and *5H*. It is shown that the most stable tautomer is *2H*, tautomer *3H* has intermediate energy and the *5H* has the highest energy. This compound provides a striking counter-example of the generally held view that the organic conjugated structure with the highest number of alternating single and double bonds is the most stable.



**R. Centore,* S. Fusco, A. Capobianco,
V. Piccialli, S. Zaccaria,
A. Peluso** 1–10

Tautomerism in the Fused N-Rich Tri-
azolotriazole Heterocyclic System 

Keywords: Nitrogen heterocycles /
Tautomerism

DOI: 10.1002/ejoc.201201653

Tautomerism in the Fused N-Rich Triazolotriazole Heterocyclic System

Roberto Centore,^{*[a]} Sandra Fusco,^[a] Amedeo Capobianco,^[b] Vincenzo Piccialli,^[a] Sabrina Zaccaria,^[a] and Andrea Peluso^[b]

Keywords: Nitrogen heterocycles / Tautomerism

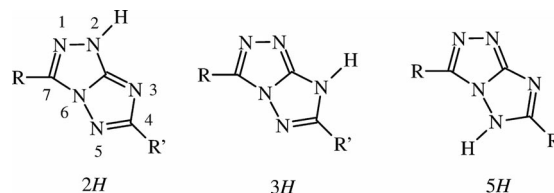
Tautomerism in the [1,2,4]triazolo[3,2-*c*][1,2,4]triazole fused aromatic system has been investigated by single-crystal X-ray analysis, UV/Vis spectroscopy and theoretical calculations on selected new heterobicycle derivatives. The reactions of 3,4-diamino-1,2,4-triazoles with acyl chlorides or acetic anhydride in pyridine at reflux led to ring closure and the fused aromatic system was obtained as the secondary amide at N2 instead of at N5 as previously reported in the literature. For the [1,2,4]triazolo[3,2-*c*][1,2,4]triazole system, three different tautomers can be present. Crystal structure

analysis showed the presence of only one tautomer or, depending on the packing, a mixture of two; theoretical calculations supported this finding, predicting that for all the investigated compounds one tautomer is energetically disfavoured with respect to the other two. The electronic absorption spectra of some compounds show a marked solvent dependence, which has been interpreted, with the help of theoretical calculations, in terms of acid/base equilibria, which are critically dependent upon the substituents at the heterobicycle.

Introduction

Heterocycles are key compounds in synthetic chemistry. In addition to their long-standing and important applications in drugs and bioactive compounds, aromatic heterocycles play a fundamental role in modern materials chemistry as building blocks of conjugated active molecules in many emerging fields of organic electronics and optoelectronics: conducting polymers,^[1] organic field-effect transistors,^[2] organic solar cells^[3] and non-linear optically active compounds.^[4] Fused aromatic heterocycles can be an interesting alternative to fused aromatic hydrocarbons^[5] in many applications in organic electronics, because the presence of heteroatoms can help to modulate the energy of the HOMO and LUMO levels as well as the electron-poor/rich nature of the compounds. In this context, N-rich fused systems and, in particular, those containing acidic N–H groups, are potentially interesting because they are expected to be more soluble in solvents like pyridine, DMF or NMP. In addition, they can show tautomerism. Following our interest in advanced materials^[6] and bioactive compounds^[7] based on 10-electron aromatic fused heterocycles, we directed our attention towards the [1,2,4]triazolo[3,2-*c*][1,2,4]triazole fused aromatic system, for which three different tautomers

can, in principle, be expected: the *2H*, *3H* and *5H* tautomers (chemical diagrams of the tautomers and atomic numbering used throughout the paper for the [1,2,4]triazolo[3,2-*c*][1,2,4]triazoles are shown in Scheme 1).



Scheme 1. Tautomers of [1,2,4]triazolo[3,2-*c*][1,2,4]triazole.

A comprehensive experimental and theoretical analysis of this fused heterocycle is missing. One detailed account of the synthetic procedures was given in the 1960s but without any comment on its tautomerism (only the *5H* isomer was assumed).^[8] Subsequently, tautomerism of the system was formally acknowledged,^[9] but only the *3H* and *5H* tautomers were considered. Two subsequent papers^[10] reported semi-empirical theoretical calculations of the three tautomers for the simple heterobicycle system with $R = R' = H$, henceforth *HH*, with measurement of the electric dipole moments. Finally, in the few, more recent papers in which the fused heterobicycle appeared, there was no mention of tautomerism.^[11]

In this paper we present the synthesis of several new triazolo[3,2-*c*]triazoles with a detailed crystallographic, spectroscopic and up-to-date theoretical analysis focused on tautomerism and regiochemistry.

[a] Department of Chemical Sciences, University of Naples "Federico II",

Via Cinthia, 80126 Napoli, Italy

Fax: +39-081674090

E-mail: roberto.centore@unina.it

Homepage: <https://www.docenti.unina.it/roberto.centore>

[b] Dipartimento di Chimica e Biologia, Università di Salerno, Via Ponte don Melillo, 84084 Fisciano (SA), Italy

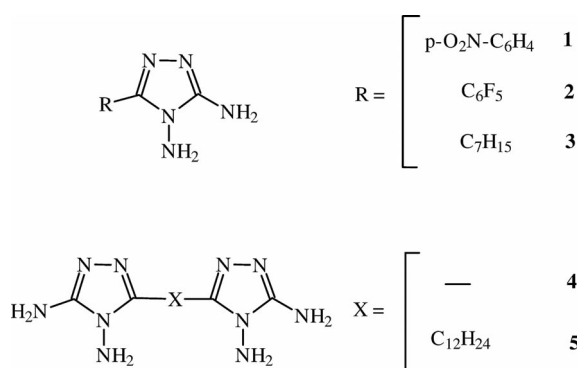
Supporting information for this article is available on the WWW under <http://dx.doi.org/10.1002/ejoc.201201653>.

Results and Discussion

Regiochemistry

According to the literature,^[8] triazolo[3,2-*c*]triazoles can be prepared by the reaction of 3,4-diamino-1,2,4-triazoles with acyl chlorides or acetic anhydride ($R' = \text{CH}_3$) in pyridine at reflux. By using a large excess of the acylating agent, the fused system was obtained with the secondary amide at N5 from which, by basic hydrolysis, the final compound was obtained (the *5H* tautomer). However, it must be acknowledged that the only analytical data reported in ref.^[8] are elementary analyses, which, of course, do not provide real proof of either the regiochemistry of amide formation or which tautomer is formed upon hydrolysis of the secondary amide. In a similar manner, in subsequent reports,^[9,11] formation of the *3H* or *5H* tautomer is claimed, at least in the chemical diagrams reported, again without any experimental proof.

In this paper we have prepared several new triazolo[3,2-*c*]triazoles starting from the diaminotriazoles reported in Scheme 2. These, in turn, were prepared according to a procedure described by us in a preceding paper.^[12]



Scheme 2. 3,4-Diamino-1,2,4-triazoles used in the synthesis of the new triazolo[3,2-*c*]triazoles.

In a first experiment we treated, according to ref.^[8], diaminotriazole **1** with excess acetic anhydride. After appropriate workup (see the Exp. Sect.) we isolated a crystalline product in high yield (79%); its ¹H NMR spectrum indicated the formation of the amidated heterobicycle, as expected. However, the X-ray analysis (Figure 1) revealed that the amide was formed at the N2 atom, which is in contrast to ref.^[8] and in agreement with the indirect assignment proposed in ref.^[10b] This compound will be denoted henceforth as TT1A. The molecular structure of TT1A is substantially flat, as indicated by the dihedral angle between the average planes of the bicycle and the phenyl ring, which is 2.3(1)°.

The regiochemistry of the amide formation can be explained simply on the grounds that N2 is the least sterically encumbered position of the heterobicycle (but see below for the discussion on the packing and electronic effects). The reactivity of non-conjugated bis(diaminotriazoles) proved to be essentially the same as the monodiaminotriazoles. For

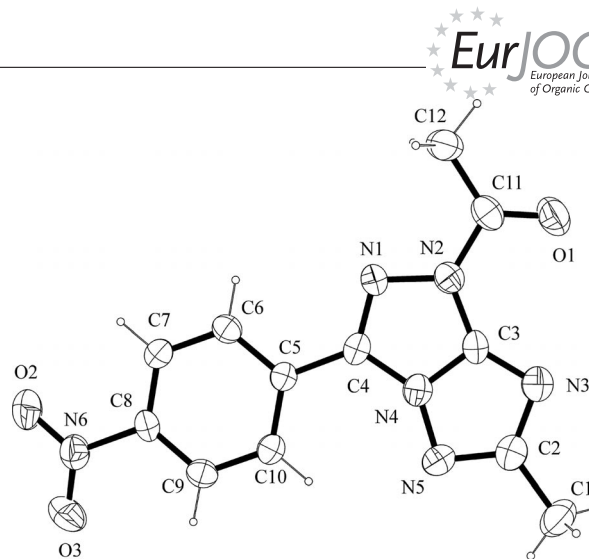


Figure 1. Ortep diagram of TT1A. Thermal ellipsoids are drawn at the 50% probability level. Selected bond lengths [Å], bond angles [°] and torsion angles [°]: C2–N3 1.366(4), C3–N2 1.374(4), C3–N3 1.332(4), C3–N4 1.343(4), C4–N1 1.323(4), N1–N2 1.391(4), N4–N5 1.367(4), N2–C3–N3 141.7(4), C4–N4–N5 140.9(3), C10–C5–C4–N1 –177.4(3), O1–C11–N2–N1 –175.4(3).

example, treatment of bis(diaminotriazole) **5** with excess acetic anhydride afforded the diamidated-bis(heterobicycle) (see the Exp. Sect.).

In the sole case of bitriazole **4**, heating at reflux in excess acetic anhydride did not afford the diamidated-bis(heterobicycle) but the tetra-acetamide of the bitriazole (TAM) in 80% yield (Figure 2).

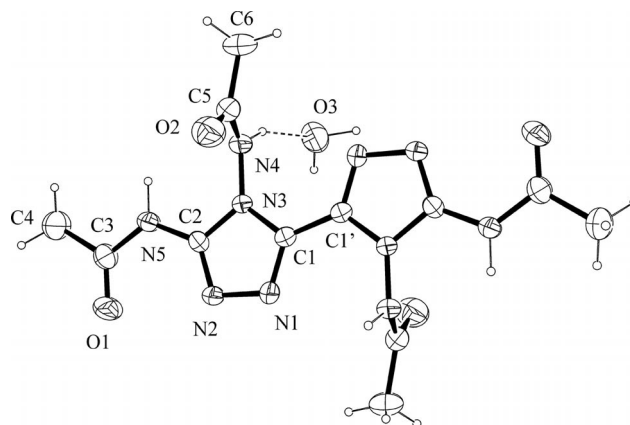


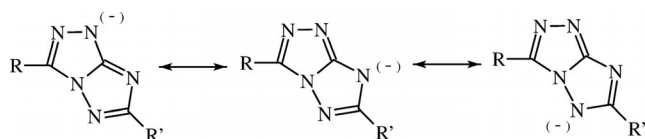
Figure 2. X-ray structure of 3,3',4,4'-tetraacetamidobi-1,2,4-triazol-5-yl dihydrate (TAM). Thermal ellipsoids are drawn at the 50% probability level. Selected bond lengths [Å], bond angles [°] and torsion angles [°]: C1–C1' 1.447(6), N1–C1–C1' 126.3(4), N3–C1–C1' 123.9(4), N1–C1–C1'–N1' –180.0(4), N3–C2–N5–C3 176.4(3), C2–N3–N4–C5 99.5(4).

Solid-State Structures of the Tautomers

Basic hydrolysis of N2-amidated heterobicycles afforded the N–H heterobicycles. These can also be obtained in two steps by reaction of the diaminotriazole with 1 equiv. of the acylating agent, obtaining the amino-hydrazide that can be isolated and cyclized in the presence of a dehydrating agent,

FULL PAPER

for example, POCl₃ (see the Exp. Sect.). N–H heterobicycles are generally soluble in pyridine, DMF and DMSO. In all the cases that we have investigated, the ¹H NMR spectra recorded in [D₆]DMSO show the resonance of the N–H proton as a broad singlet at high δ values, δ = 13–14 ppm, which indicates that the proton is very acidic. In fact, the deprotonated form of the heterobicycle is highly resonance-stabilized (Scheme 3).



Scheme 3. Resonance forms of the deprotonated heterobicycle.

In two cases we were successful in growing single crystals of the N–H heterobicycle suitable for X-ray analysis. In the first case, compound TT2 (R = C₆F₅, R' = CH₃ in Scheme 1, Figure 3), the 2*H* tautomer is obtained unambiguously. It is worth noting that in previous experimental investigations,^[8,9,11] the 2*H* tautomer had never been considered for this fused heterocycle even though it was proposed as the most stable in early theoretical investigations.^[10]

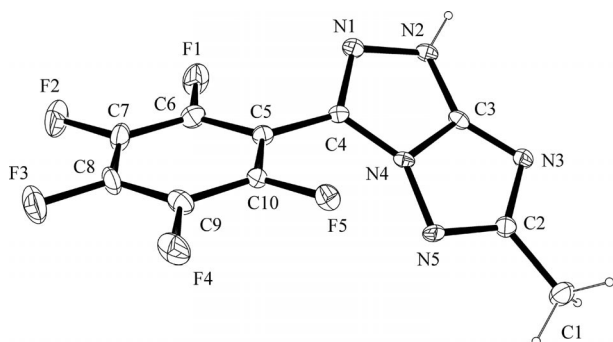


Figure 3. X-ray molecular structure of 4-methyl-7-(pentafluorophenyl)-2*H*-[1,2,4]triazolo[3,2-*c*][1,2,4]triazole (TT2). Thermal ellipsoids are drawn at the 30% probability level. Selected bond lengths [Å], bond angles [°] and torsion angles [°]: C2–N3 1.377(4), C2–N5 1.341(4), C3–N2 1.341(4), C3–N3 1.313(4), C3–N4 1.355(4), C4–N1 1.322(4), N1–N2 1.367(4), N4–N5 1.378(3), N2–C3–N3 141.7(3), C4–N4–N5 142.5(3), C10–C5–C4–N1 –138.5(3).

The molecular conformation of TT2 is determined by the twist around the C4–C5 bond, which produces a dihedral angle of 40.3(1)° between the average planes of the bicycle and the pentafluorophenyl ring; the twist is probably related to the close contacts between F5 and N4 and N5 [F5⋯N4 2.876(4) Å, F5⋯N5 2.868(3) Å].

In the second case, compound TT3 (R = C₇H₁₅, R' = *p*-O₂N-C₆H₄ in Scheme 1, Figure 4), the pattern of tautomerism emerging from the crystallographic analysis is more subtle. In fact, the X-ray analysis gives clear evidence of the hydrogen atom bonded to N2, but there is also evidence, from low temperature data collections from different crystal specimens, of another hydrogen atom bonded to N3, the two hydrogen atoms having a weight ratio of approximately

0.8:0.2. Therefore we can conclude that crystals of TT3 contain a mixture of 2*H* and 3*H* tautomers, with the 2*H* isomer prevailing over the 3*H* tautomer.

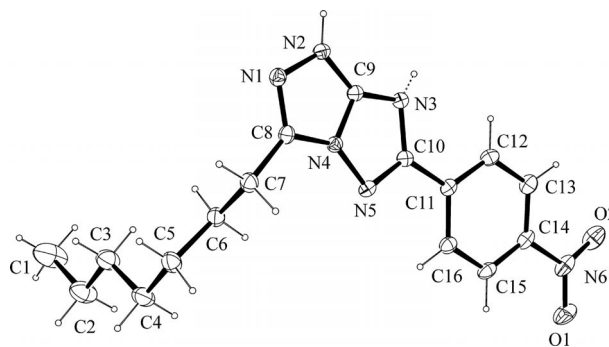


Figure 4. X-ray molecular structure of 7-*n*-heptyl-4-(4-nitrophenyl)-2(3)*H*-[1,2,4]triazolo[3,2-*c*][1,2,4]triazole (TT3). Thermal ellipsoids are drawn at the 30% probability level. Selected bond lengths [Å], bond angles [°] and torsion angles [°]: C10–N3 1.376(3), C10–N5 1.332(3), C9–N2 1.337(3), C9–N3 1.328(3), C9–N4 1.342(3), C8–N1 1.307(3), N1–N2 1.391(2), N4–N5 1.370(2), N2–C9–N3 141.9(2), C8–N4–N5 140.8(2), C3–C4–C5–C6 64.2(3), C6–C7–C8–N4 67.1(3), C16–C11–C10–N3 174.5(2).

In TT3, the dihedral angle between the bicycle and the phenyl ring is 7.6(1)° and the alkyl chain is out of the plane of the bicycle.

It is possible, in principle, that the relative stability of the three tautomers of the triazolotriazole system is influenced by steric factors. However, in the 3*H* and 5*H* tautomers of TT3, only a loose 1,6 contact between hydrogen atoms would be present if the phenyl ring is coplanar with the heterobicycle.^[13] Analogously, for TT2, the 3*H* tautomer would not suffer any apparent steric problem.

Packing factors could also lead to one tautomer being favoured over the others. In fact, the compounds shown in Figures 3 and 4 have a bent shape; if the H atom is bonded to N2 or N3, it is in the convex part of the molecule, pointing outwards, whereas in the 5*H* tautomer, the H atom is in the concave part of the molecule and is more hidden. These arguments can be relevant because the packing of the compounds is likely driven by the formation of N–H⋯N hydrogen bonds.

In the crystal packing of TT3, hydrogen-bonded chains are formed with both the donor and the acceptor in the convex part of the molecule (N2–H and N3 in the case of the predominant 2*H* tautomer and N3–H and N2 in the case of the 3*H* tautomer; Figure 5). It is worth noting that the crystal packing of TT3 is invariant (metrically) by the exchange of the 2*H* and 3*H* tautomers; this means that, in principle, both can be present in the same crystal.

In the hydrogen-bonded chains formed by TT2 (Figure 6), the N2–H donor is bonded to the N5 acceptor of another molecule, producing a convex-into-concave arrangement that, metrically, could also have been produced equally well with the hydrogen bonded to N5 and N2 as the acceptor (5*H* tautomer). However, the fact that no trace of the 5*H* tautomer was detected in the X-ray analysis of TT2 strongly suggests that the energy of the 5*H* tautomer

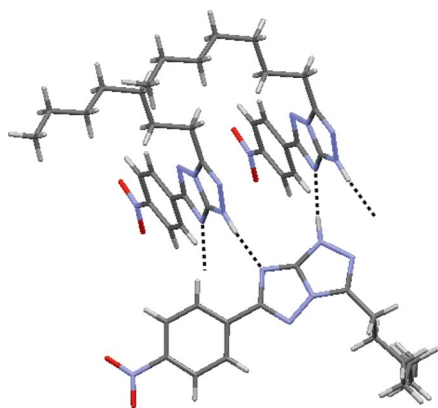


Figure 5. Hydrogen-bonded chains in the crystal packing of TT3. Only the most abundant *2H* tautomer is shown for clarity. Structural data of the hydrogen bond: N2–H2...N3': 0.90(3), 1.96(3), 2.849(3) Å, 176(3)°; $i = 1 - x, 1/2 + y, 1/2 - z$.

is considerably higher than *2H* and *3H*. Thus, the relative energies of the three tautomers, as inferred by the X-ray structures, are $E_{5H} \gg E_{3H} > E_{2H}$.

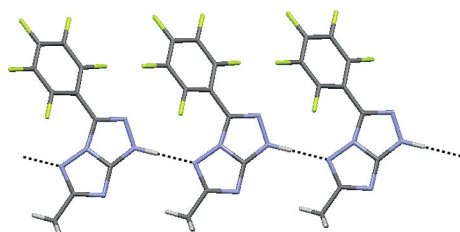


Figure 6. Hydrogen-bonded chains in the crystal packing of TT2. Structural data of the hydrogen bond: N2–H2...N5': 0.90(4), 1.93(4), 2.824(4) Å, 178(3)°; $i = -1 + x, y, z$.

Theoretical and Spectroscopic Analysis

The tautomerism of [1,2,4]triazolo[3,2-*c*][1,2,4]triazole was investigated theoretically early with reference to the most simple HH compound.^[10] Semi-empirical computations indicated that the *2H* tautomer is the most stable, followed by *3H* and *5H*, the latter having a significantly higher energy. We have theoretically investigated the tautomerism in TT1 ($R = p\text{-O}_2\text{N-C}_6\text{H}_4$, $R' = \text{CH}_3$ in Scheme 1), TT2 and TT3, as well as compound HH, which is free from the steric and electronic effects of substituents, for comparison.

The geometries of the *2H*, *3H* and *5H* tautomers of HH were fully optimized at the HF, DFT (B3LYP and BMK functionals) and MP2 levels of theory. To consider the effects of a polar environment, geometry optimizations were carried out both in the gas phase and in solution, using in the latter case the polarizable continuum model (PCM). The standard parameters of DMSO were employed to mimic polar environments. The 6-31+G** basis set was adopted in this first set of computations. Independently of the method, planar equilibrium geometries were found for the *2H* and *3H* tautomers (C_s symmetry), with the *5H* tautomer exhibiting strong pyramidalization at the N5 nitrogen

and to a lesser extent at N6, possibly due to the fact that only *5H* possesses adjacent nitrogen atoms (N5 and N6) with formal sp^3 hybridization. The computed relative energies are reported in Table 1 and the calculated dipole moments are discussed in the Supporting Information.

Table 1. Relative energies of the *2H*, *3H* and *5H* tautomers of HH predicted at different levels of theory both in the gas phase and in polar solvent (DMSO, in parentheses).^[a]

	HF	E_{rel} [kcal/mol]		MP2 ^[b]
		B3LYP	BMK	
<i>2H</i>	0.0 (0.0)	0.0 (0.0)	0.0 (0.0)	0.0 (0.0)
<i>3H</i>	10.4 (4.7)	9.3 (4.1)	9.4 (4.0)	8.5 (3.3)
<i>5H</i>	23.2 (14.2)	21.6 (12.9)	22.9 (13.5)	21.7 (13.1)
<i>5Hp</i> ^[c]	25.8 (14.8)	22.6 (13.0)	23.9 (13.5) ^[d]	23.1 (13.3)

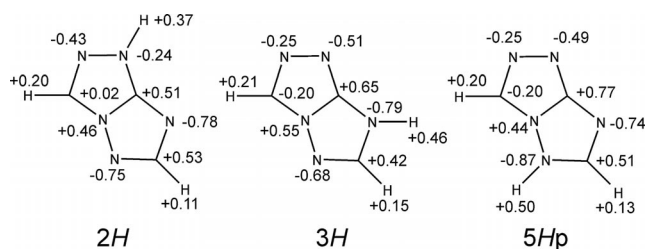
[a] Relative energies were calculated by using the 6-31+G** basis set. [b] The frozen core (FC) approximation was used in MP2 computations. [c] C_s symmetry imposed (planar geometry). [d] Equilibrium geometry of *5H* tautomer is predicted to be planar by PCM computations at the BMK level.

The *2H* tautomer is predicted to be much more stable than the *3H* and *5H* tautomers in the gas phase, *5H* having an energy more than 20 kcal/mol greater than *2H*. The Hartree–Fock relative energies are in good agreement with those determined by MP2, which indicates that the stability of tautomers cannot be ascribed to correlation effects. HH is a 10-electron aromatic system in which loss of planarity could reduce conjugation, thus the geometry of *5H* was also optimized with the constraint of planarity to evaluate the extent to which π conjugation affects the overall stability. The resulting stationary point *5Hp* possesses only one imaginary frequency corresponding to the normal coordinate for the pyramidalization of N5. Computations predict a loss of 1–3 kcal/mol, depending on the method used, in going from pyramidal to planar *5H*, a very small contribution compared with the energy difference between *2H* and *5H*, which indicates that the high energy of *5H* is not due to loss of conjugation.

The results in Table 1 show that the relative energies of both the *3H* and *5H* tautomers are lower in a polar environment; *3H* is stabilized by around 5 kcal/mol with respect to the gas phase according to all methods, and *5H* by around 10 kcal/mol. Computations employing more accurate methods (coupled cluster) and extended basis sets confirmed the results in Table 1 (see the Supporting Information).

The charge distributions predicted by the HF computations are shown in Scheme 4. An increase in negative charge on C7 is predicted on going from *2H* to *3H* and *5H*; this trend suggests that substitution at C7 with an electron-withdrawing group should result in the enhanced stability of *3H* and *5H* compared with *2H*. In contrast, the charge on C4 (when summed with the charge on H4) is rather insensitive to tautomerism.

On the basis of the preceding results, TT1, TT2 and TT3 were studied at the DFT/6-31+G** level of theory both in the gas phase and in polar solvents, ethanol and water, by using the PCM method. The computed relative energies of the *2H*, *3H* and *5H* tautomers of TT1, TT2 and TT3 are



Scheme 4. Charge distribution (HF/QZVPP) in the tautomers of HH.

reported in Table 2 and the calculated dipole moments are discussed in the Supporting Information. The equilibrium geometries of the *2H* tautomers of TT2 and TT3 closely resemble those obtained by X-ray diffraction. Pyramidalization of the N5 nitrogen was found for the *5H* tautomer in all three compounds in the gas phase as well as in polar solvent.

Table 2. Computed relative energies, in reference to tautomer *2H*, of tautomers *3H* and *5H* of TT1, TT2 and TT3.^[a]

	E_{rel} [kcal/mol]					
	Gas		EtOH		H_2O	
	<i>3H</i>	<i>5H</i>	<i>3H</i>	<i>5H</i>	<i>3H</i>	<i>5H</i>
TT1	6.9	21.4	1.2	13.0	0.9	12.4
TT2	6.8	17.3	2.3	11.2	2.1	10.8
TT3	14.1	25.5	8.6	17.5	8.3	16.9

[a] Calculated at the (PCM)BMK/6-31+G** level. Relative energies predicted by B3LYP computations are given in the Supporting Information.

The relative energies in Table 2 suggest that for TT1 and TT2, a small fraction of the tautomer *3H* could be present in the solution of polar solvents. Indeed, the UV/Vis spectra of TT1 and TT2 recorded in ethanol and ethanol/water mixtures (Figure 7 and Figure 8) show a significant solvent dependence that could be ascribed to the presence of two tautomers in solution, whereas for TT3 no significant changes can be observed (Figure 9).

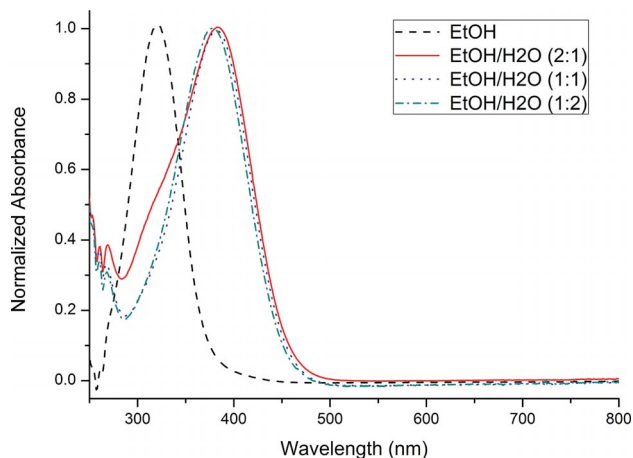


Figure 7. UV/Vis spectra of TT1.

The absorption spectrum of TT1 (Figure 7) in EtOH exhibits an intense band with a maximum at 321 nm. On addition of water, the band at 321 nm becomes a shoulder of

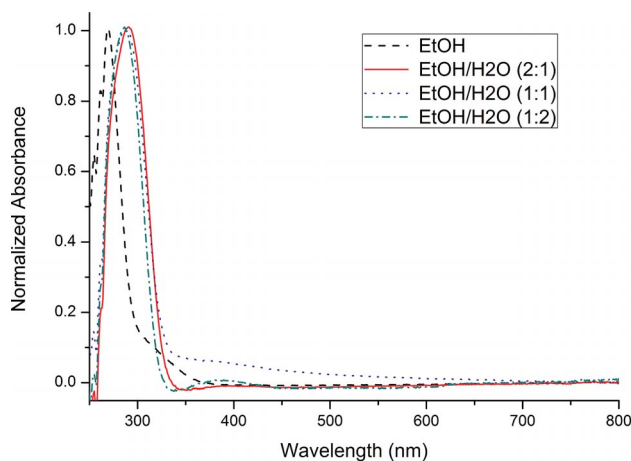


Figure 8. UV/Vis spectra of TT2.

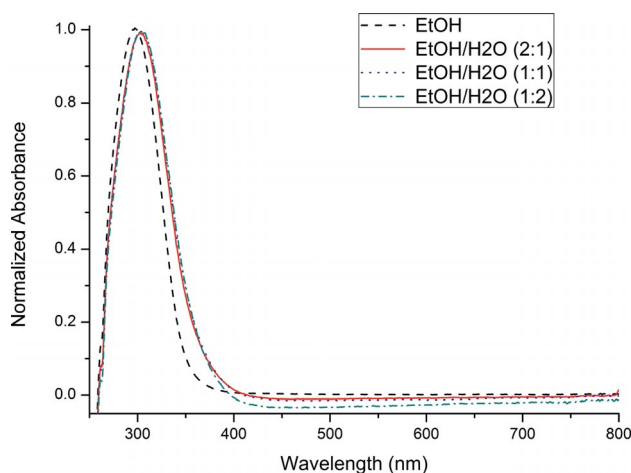


Figure 9. UV/Vis spectra of TT3.

a new band with a maximum at a longer wavelength (382 nm). By increasing the concentration of water, the shoulder at 321 nm weakens and the higher wavelength band gains intensity. The spectra recorded for TT2 (Figure 8) are similar to those of TT1, but the maxima of the two bands are closer to each other (269 and 297 nm).

This spectroscopic behaviour could be explained by an increase in the concentration of the *3H* tautomer in going from ethanol to water/ethanol mixtures, but this hypothesis is not supported by TD-DFT computations, the results of which are reported in Table 3. No substantial changes in absorption wavelengths and intensities are predicted on going from the *2H* to the *3H* tautomer for the three compounds. The most intense transition for TT1 in EtOH is predicted to be at 319 nm for *2H* and 337 nm for *3H*. No significant solvatochromic shift is predicted for a change in solvent from ethanol to water for both tautomers. We have thus considered the hypothesis that acid/base equilibria could be responsible for the observed behaviour. TD-DFT computations were carried out for the conjugate bases of the three compounds. An intense transition, centred at 420 nm, is predicted for the conjugate base of TT1, well compatible with the wavelength of the most intense band

Table 3. Predicted wavelengths (λ) and oscillator strengths (f) of the most intense transitions of tautomers *2H* and *3H* and of the conjugate base of TT1, TT2, and TT3 in H₂O and EtOH (in parentheses).^[a]

	<i>2H</i>		<i>3H</i>		Conj. base	
	λ [nm]	f	λ [nm]	f	λ [nm]	f
TT1	319(319)	0.60(0.60)	337(337)	0.67(0.68)	420(424)	0.64(0.65)
	234(234)	0.05(0.05)	221(221)	0.19(0.19)	251(252)	0.10(0.09)
	221(221)	0.06(0.06)			249(250)	0.17(0.17)
	215(215)	0.10(0.11)			202(203)	0.08(0.09)
TT2	260(260)	0.30(0.30)	261(261)	0.42(0.43)	314(317)	0.32(0.33)
	215(215)	0.06(0.06)	217(217)	0.09(0.09)	215(216)	0.10(0.10)
	211(211)	0.12(0.12)	212(213)	0.07(0.07)		
TT3	304(304)	0.73(0.74)	315(316)	0.07(0.07)	340(342)	0.68(0.69)
	206(205)	0.19(0.19)	295(295)	0.67(0.68)	250(252)	0.08(0.08)
			207(207)	0.08(0.06)	218(218)	0.23(0.23)
			205(205)	0.15(0.17)		

[a] Calculated at the PCM/TD-BMK/6-31+G** level.

observed in ethanol/water mixtures. Indeed, as is also evidenced by the ¹H NMR spectra (see the discussion preceding Scheme 3 and also Scheme S1 in the Supporting Information), TT1 is estimated to be more acidic than the parent HH owing to both resonance and inductive effects. The latter argument can be invoked for TT2 for which theoretical computations predict an intense transition at 260 nm for both *2H* and *3H* (both in ethanol and water), which compares well with the λ_{max} (269 nm) observed in ethanol. The most intense transition for the conjugated base is predicted at around 315 nm in both solvents and indeed a band peaked at 297 nm is observed in the spectra recorded in ethanol/water mixtures.

The fact that the absorption spectrum of TT3 does not show significant changes in passing from ethanol to ethanol/water mixtures can be ascribed to the expected (and also predicted) lower acidity of TT3 compared with TT1 and TT2.

Conclusions

[1,2,4]Triazolo[3,2-*c*][1,2,4]triazole is a 10-electron aromatic N-rich fused heterocycle that can exist in three different tautomers: *2H*, *3H* and *5H*. This heterocycle provides a striking counter-example of the generally held view that the organic conjugated structure with the highest number of alternating single and double bonds is the most stable. In fact, although the *5H* tautomer would fulfil such a requirement, it is in fact the least stable tautomer. Electronic absorption spectra have shown that the acidity of [1,2,4]triazolo[3,2-*c*][1,2,4]triazole derivatives is critically dependent upon the substituents on the heterobicycle.

Experimental Section

Materials and Methods: All reagents were analytical grade and used without further purification. Melting points were determined by temperature-controlled optical microscopy (Zeiss Axioskop polarizing microscope equipped with a Mettler FP90 heating stage). NMR spectra were recorded with Gemini or Varian spectrometers operating at 200 MHz in [D₆]DMSO, [D₅]Py or CDCl₃. ¹H NMR chemical shifts are referenced to the residual signals of the solvent:

DMSO (δ = 2.50 ppm), Py (δ = 7.22, 7.58, 8.74 ppm) or CHCl₃ (δ = 7.26 ppm). ¹³C NMR chemical shifts are referenced to the solvent ([D₆]DMSO: δ = 39.51 ppm; [D₅]Py: δ = 123.87, 135.91, 150.35 ppm). ESI mass spectrometric analyses were recorded with an Applied Biosystems API 2000 mass spectrometer equipped with an electrospray source used in the positive mode. UV/Vis absorption spectra were measured with a Jasco V560 spectrophotometer.

Syntheses: Reactions of the diaminotriazoles with acetic anhydride, as well as the basic hydrolysis of the amidated products were performed in accord with literature procedures,^[8] so they will be described in detail for only one system.

2-Acetyl-4-methyl-7-(4-nitrophenyl)-[1,2,4]triazolo[3,2-*c*][1,2,4]triazole (TT1A): 3,4-Diamino-5-(*p*-nitrophenyl)-1,2,4-triazole (0.500 g, 2.28 mmol) was suspended in acetic anhydride (10 mL). The mixture was heated at reflux for 3 h. The resulting solution was cooled to room temperature and poured into water (70 mL). The pale-pink solid formed was recovered by filtration and recrystallized from dimethylformamide/water, yield 0.510 g (79%), m.p. 203 °C. ¹H NMR (200 MHz, [D₅]Py): δ = 2.63 (s, 3 H), 2.81 (s, 3 H), 8.43 (d, J = 9.2 Hz, 2 H), 8.60 (d, J = 8.6 Hz, 2 H) ppm. MS (ESI): calcd. for C₁₂H₁₀N₆O₃ 286.2 [M]⁺; found 309.0 [M + Na]⁺.

1,12-Bis(2-acetyl-4-methyl-7-(4-nitrophenyl)-[1,2,4]triazolo[3,2-*c*][1,2,4]triazole-7-yl)do-decane: Yield 77%, m.p. 150 °C. ¹H NMR (200 MHz, CDCl₃): δ = 1.27–1.36 (m, 12 H), 1.65 (m, 4 H), 1.89 (m, 4 H), 2.53 (s, 6 H), 2.70 (s, 6 H), 2.95 (t, 4 H) ppm. ¹³C NMR (50 MHz, [D₅]Py): δ = 15.5 (2 Me), 22.1 (2 acetyl Me), 25.2, 25.7, 29.3, 29.4, 29.7, 29.8 (12 CH₂), 139.5, 143.0, 155.4 (6 C_{triaz}), 169.6 (2 CO) ppm. MS (ESI): calcd. for C₂₄H₃₆N₁₀O₂ 496.6 [M]⁺; found 519.2 [M + Na]⁺.

4-Methyl-7-(4-nitrophenyl)-2H-[1,2,4]triazolo[3,2-*c*][1,2,4]triazole (TT1): 2-Acetyl-4-methyl-7-(4-nitrophenyl)triazolo[3,2-*c*]triazole (0.370 g, 1.29 mmol) was suspended in 5% KOH (20 mL). The mixture was heated at reflux for 1 h to give a red solution. The solution was cooled to room temperature and acidified to pH 4 with 0.1 M HCl. A white product was obtained that was recrystallized from DMF, yield 0.252 g (80%), m.p. 319 °C (decomp.). λ_{max} (EtOH) = 321 nm; ϵ_{max} = 1.82 × 10⁴ L mol⁻¹ cm⁻¹. ¹H NMR (200 MHz, [D₆]DMSO): δ = 2.41 (s, 3 H), 8.43 (m, 4 H), 14.2 (br. s, 1 H) ppm. ¹³C NMR (50 MHz, [D₆]DMSO): δ = 15.05 (Me), 124.6, 126.35, 131.1, 135.6 (C_{Ph}), 147.9, 157.65, 168.3 (C_{triaz}) ppm. MS (ESI): calcd. for C₁₀H₈N₆O₂ 244.2 [M]⁺; found 245.0 [M + H]⁺, 267.0 [M + Na]⁺.

4-Methyl-7-(pentafluorophenyl)-2H-[1,2,4]triazolo[3,2-*c*][1,2,4]triazole (TT2): Yield: 75%, m.p. 212 °C. λ_{max} (EtOH) = 269 nm; ϵ_{max}

$= 8.8 \times 10^3 \text{ L mol}^{-1} \text{ cm}^{-1}$. $^1\text{H NMR}$ (200 MHz, $[\text{D}_6]$ DMSO): $\delta = 2.36$ (s, 3 H), 14.3 (br. s, 1 H) ppm. $^{13}\text{C NMR}$ (50 MHz, $[\text{D}_6]$ -DMSO): $\delta = 14.6$ (Me), 126.2, 135.1, 140.2, 142.0 (C_{Ph}), 147.0, 156.9, 167.2 (C_{triaz}) ppm. MS (ESI): calcd. for $\text{C}_{10}\text{H}_4\text{N}_5\text{F}_5$ 289.2 $[\text{M}]^+$; found 290.0 $[\text{M} + \text{H}]^+$, 311.9 $[\text{M} + \text{Na}]^+$.

1,12-Bis(4-methyl-2H-[1,2,4]triazolo[3,2-c][1,2,4]triazol-7-yl)dodecane: Yield: 64%, m.p. 236 °C. $^1\text{H NMR}$ (200 MHz, $[\text{D}_5]$ Py): $\delta = 1.24$ (m, 16 H), 1.97 (m, 4 H), 2.59 (s, 6 H), 3.03 (tr, 4 H) ppm. MS (ESI): calcd. for $\text{C}_{20}\text{H}_{32}\text{N}_{10}$ 412.5 $[\text{M}]^+$; found 413.2 $[\text{M} + \text{H}]^+$.

3-Amino-4-(4-nitrophenylbenzamido)-5-*n*-heptyl-1,2,4-triazole: 3,4-Diamino-5-*n*-heptyl-1,2,4-triazole (0.500 g, 2.53 mmol) was dissolved in pyridine (20 mL). 4-Nitrobenzoyl chloride (0.493 g, 2.66 mmol) was added to the solution. The suspension was heated at reflux for 3 h under magnetic stirring and then the solution was cooled to room temperature and poured into water (50 mL). A white solid was obtained that was recovered by filtration and recrystallized from DMF, yield 0.389 g (45%), m.p. 270 °C. $^1\text{H NMR}$ (200 MHz, $[\text{D}_6]$ DMSO): $\delta = 0.88$ (t, 3 H), 1.30 (m, 8 H), 1.70 (quint., 2 H), 2.69 (t, 2 H), 5.78 (s, 2 H), 8.33 (m, 5 H) ppm. $^{13}\text{C NMR}$ (50 MHz, $[\text{D}_6]$ DMSO): $\delta = 13.9$ (Me), 22.1, 23.7, 25.7, 28.3, 28.4, 31.1 (6 CH_2), 123.15, 129.9, 143.4, 148.9, 150.6, 152.2 (C_{Ph} and C_{triaz}), 169.4 (CO) ppm.

4-Nitrophenyl-7-*n*-heptyl-2(3)-H-[1,2,4]triazolo[3,2-c][1,2,4]triazole (TT3): 3-Amino-4-(4-nitrophenylbenzamido)-5-*n*-heptyl-1,2,4-triazole (0.250 g, 0.722 mmol) was suspended in POCl_3 (15 mL). The suspension was heated at reflux whilst stirring for 4 h. The resulting solution was added dropwise into cold water (50 mL) whilst stirring. A white solid formed, which was recovered by filtration and recrystallized from DMF/water, yield 0.202 g (85%), m.p. 187 °C. λ_{max} (EtOH) = 297 nm; $\epsilon_{\text{max}} = 1.44 \times 10^4 \text{ L mol}^{-1} \text{ cm}^{-1}$. $^1\text{H NMR}$ (200 MHz, $[\text{D}_6]$ DMSO): $\delta = 0.83$ (m, 3 H), 1.2–1.7 (m, 8 H), 1.80 (m, 2 H), 2.95 (t, 2 H), 8.32 (m, 4 H), 13.6 (br. s, 1 H) ppm. $^{13}\text{C NMR}$ (50 MHz, $[\text{D}_6]$ DMSO): $\delta = 13.9$ (Me), 22.0, 24.3, 25.1, 28.15, 28.25, 31.0 (6 CH_2), 124.1, 127.4, 137.6, 139.7 (C_{Ph}), 148.0, 157.2, 165.9 (C_{triaz}) ppm. MS (ESI): calcd. for $\text{C}_{16}\text{H}_{20}\text{N}_6\text{O}_2$ 328.4 $[\text{M}]^+$; found 329.1 $[\text{M} + \text{H}]^+$.

3,3',4,4'-Diacetamidobi-1,2,4-triazol-5-yl: Finely ground 3,4-diamino-5-(3,4-diamino-1,2,4-triazol-5-yl)-1,2,4-triazole (0.525 g, 2.68 mmol) was suspended in acetic anhydride (20 mL) at reflux for 4 h. The mixture was cooled to room temperature and the white solid was filtered and recrystallized from water/ethanol (90:10 v/v), yield 0.781 g (80%), m.p. 280 °C. $^1\text{H NMR}$ (200 MHz, $[\text{D}_6]$ -

DMSO): $\delta = 2.01$ (s, 6 H), 2.09 (s, 6 H), 10.56 (s, 2 H), 11.47 (s, 2 H) ppm. $^{13}\text{C NMR}$ (50 MHz, $[\text{D}_6]$ DMSO): $\delta = 20.6$, 22.8 (4 Me), 140.9, 148.9 (4 C_{triaz}), 169.2, 169.5 (4 CO) ppm. MS (ESI): calcd. for $\text{C}_{12}\text{H}_{16}\text{N}_{10}\text{O}_4$ 364.3 $[\text{M}]^+$; found 387.1 $[\text{M} + \text{Na}]^+$.

X-ray Analysis: All crystal structure determinations were measured with a Bruker-Nonius KappaCCD diffractometer equipped with an Oxford Cryostream 700 apparatus using graphite-monochromated MoK_α radiation ($\lambda = 0.71073 \text{ \AA}$). Reduction of data and semi-empirical absorption corrections were performed by using the SADABS program.^[14] The structures were solved by direct methods (SIR97 program^[15]) and refined by the full-matrix least-squares method on F^2 using the SHELXL-97 program^[16] with the aid of the program WinGX.^[17] Hydrogen atoms bonded to carbon were generated stereochemically and refined by the riding model, those bonded to nitrogen in TT2 and TT3 were found in difference Fourier maps and their coordinates were refined. Crystal and refinement data are summarized in Table 4. The crystal packing analysis was performed by using the Mercury program.^[18]

CCDC-904802 (for TAM), -904803 (for TT1A), -904804 (for TT2) and -904805 (for TT3) contain the supplementary crystallographic data for this paper. These data can be obtained free of charge from The Cambridge Crystallographic Data Centre via www.ccdc.cam.ac.uk/data_request/cif.

Computational Details: Geometry optimizations at the Hartree–Fock (HF), density functional theory (DFT, B3LYP and BMK hybrid functionals were used), and Møller–Plesset perturbation theory up to second-order (MP2) levels were carried out in conjunction with the 6-31+G** basis set. The near Hartree–Fock limit (NHF) of HH was estimated by optimizing the geometries with the quadruple- ζ QZVPP basis set including up to g functions for C and N and up to f functions for H atoms. Effects due to polarization of the solvent were modelled by the polarizable continuum model (PCM).^[19] The nature of all stationary points (both in vacuo and in the solution phase) was verified by computing the eigenvalues of the Hessian matrix. To find the real absolute minimum, geometry optimizations of the TT*n* compounds were preceded by optimized potential energy scans in which all the internal coordinates were optimized but the angular variable ω , the dihedral angle formed by the bicycle and the aryl planes, which was held fixed in every partial optimization and varied in the range 0–180° in steps of two degrees. For TT3 the *n*-C₇H₁₅ substituent was replaced by an ethyl group in all computations. The adopted computational approach was validated by performing several test computations at the CC2,

Table 4. Crystallographic data for the studied compounds.

	TT1A	TAM	TT2	TT3
Formula	$\text{C}_{12}\text{H}_{10}\text{N}_6\text{O}_3$	$(\text{C}_{12}\text{H}_{16}\text{N}_{10}\text{O}_4) \cdot 2(\text{H}_2\text{O})$	$\text{C}_{10}\text{H}_4\text{F}_5\text{N}_5$	$\text{C}_{16}\text{H}_{20}\text{N}_6\text{O}_2$
<i>M</i>	286.26	400.38	289.18	328.38
Space group	<i>Pbca</i>	<i>P2₁/c</i>	<i>P2₁/c</i>	<i>P2₁/c</i>
<i>a</i> [Å]	12.606(4)	9.231(5)	5.991(3)	18.594(6)
<i>b</i> [Å]	7.2980(10)	12.215(7)	22.035(7)	5.910(3)
<i>c</i> [Å]	27.778(2)	9.458(6)	8.670(4)	15.422(6)
β [°]	90	119.30(3)	106.83	101.13(3)
<i>V</i> [Å ³]	2555.5(9)	930.0(9)	1095.5(8)	1662.8(12)
<i>Z</i>	8	4	4	4
Density [g/cm ³]	1.488	1.430	1.753	1.312
<i>T</i> [K]	296(2)	293(2)	173(2)	173(2)
μ [mm ⁻¹]	0.112	0.116	0.173	0.091
Reflections collected	15778	4147	7837	10112
Unique reflections (<i>R</i> _{int})	2249 (0.11)	1625 (0.086)	2470 (0.061)	3652 (0.041)
<i>R</i> ₁ [<i>I</i> > 2 σ (<i>I</i>)]	0.0617	0.0642	0.0551	0.0474
<i>wR</i> ₂ (all data)	0.1580	0.1443	0.1063	0.1124

CCSD and CCSD(T) levels of computation. The results are reported in the Supporting Information. Time-dependent DFT (TD-DFT), NHF, HF, DFT and MP2 computations with the 6-31+G** basis set were carried out by using the Gaussian 09 package.^[20] Single-point computations (using MP2/6-31+G** optimized geometries) at the MP2 and coupled cluster [CC2, CCSD, CCSD(T)] levels were carried out by using the TURBOMOLE suite of programs.^[21] The extended aug-cc-pVTZ basis set was used. The frozen core approximation was employed in all post Hartree–Fock computations. The resolution of identity was employed in MP2 and coupled cluster computations with the aug-cc-pVTZ basis set. Atomic charges were computed by fitting the electrostatic potential according to the Merz–Kollman scheme.^[22] We used a similar computational approach in a recent study of the conjugation in push–pull molecules.^[23] TD-DFT computations were carried out by using the BMK functional which is known to furnish better estimates of wavelengths than B3LYP when electronic transitions between donor and acceptor groups are involved.^[24]

Supporting Information (see footnote on the first page of this article): ¹H and ¹³C NMR spectra of new products, computed dipole moments for HH, TT1, TT2 and TT3, relative energies of tautomers of HH evaluated with the NHF, MP2 and coupled cluster methods using extended basis sets, relative energies of the tautomers of TT1, TT2 and TT3 evaluated at the (PCM)B3LYP/6-31+G** level in the gas phase, ethanol and water, charge distribution (HF/QZVPP) of the conjugate base of HH.

Acknowledgments

Thanks are due to the CIMCF of the University of Naples “Federico II” for the X-ray facility. Financial support from the Ministero dell’Università e della Ricerca (MIUR) (PRIN 08 and PRIN 09) and the Compagnia di San Paolo (FARO research project) is gratefully acknowledged. The authors also thank Dr. L. Palombi for helpful discussions.

- [1] A. J. Heeger, *Chem. Soc. Rev.* **2010**, *39*, 2354–2371.
- [2] a) J. Zaumseil, H. Siringhaus, *Chem. Rev.* **2007**, *107*, 1296–1323; b) Y. Wen, Y. Liu, *Adv. Mater.* **2010**, *22*, 1–15.
- [3] J. Li, A. C. Grimsdale, *Chem. Soc. Rev.* **2010**, *39*, 2399–2410.
- [4] S. H. Jang, A. K. Jen, *Introduction to Organic Electronic and Optoelectronic Materials and Devices* (Eds.: S. S. Sun, L. R. Dalton), CRC Press, Boca Raton, FL, **2008**.
- [5] a) Y. Yamashita, *Sci. Technol. Adv. Mater.* **2009**, *10*, 1–9; b) W. H. Lee, J. Park, S. H. Sim, S. Lim, K. S. Kim, B. H. Hong, K. Cho, *J. Am. Chem. Soc.* **2011**, *133*, 4447–4454; c) R. Centore, L. Ricciotti, A. Carella, A. Roviello, M. Causà, M. Barra, F. Ciccullo, A. Cassinese, *Org. Electron.* **2012**, *13*, 2083–2093.
- [6] a) A. Carella, R. Centore, A. Fort, A. Peluso, A. Sirigu, A. Tuzi, *Eur. J. Org. Chem.* **2004**, 2620–2626; b) A. Carella, R. Centore, A. Sirigu, A. Tuzi, A. Quatela, S. Schutzmann, M. Casalboni, *Macromol. Chem. Phys.* **2004**, *205*, 1948–1954; c) R. Centore, P. Riccio, S. Fusco, A. Carella, A. Quatela, S. Schutzmann, F. Stella, F. De Matteis, *J. Polym. Sci., Part A* **2007**, *45*, 2719–2725; d) S. Fusco, R. Centore, P. Riccio, A. Quatela, G. Stracci, G. Archetti, H.-G. Kuball, *Polymer* **2008**, *49*, 186–191; e) R. Centore, S. Fusco, A. Peluso, A. Capobianco, M. Stolte, G. Archetti, H.-G. Kuball, *Eur. J. Org. Chem.* **2009**, 3535–3543.
- [7] a) G. Oliviero, J. Amato, N. Borbone, S. D’Errico, G. Piccialli, L. Mayol, *Tetrahedron Lett.* **2007**, *48*, 397–400; b) G. Oliviero, J. Amato, N. Borbone, S. D’Errico, G. Piccialli, E. Bucci, V. Piccialli, L. Mayol, *Tetrahedron* **2008**, *64*, 6475–6481; c) G. Oliviero, S. D’Errico, N. Borbone, J. Amato, V. Piccialli, G. Piccialli, L. Mayol, *Eur. J. Org. Chem.* **2010**, 1517–1524; d) G. Oliviero, S. D’Errico, N. Borbone, J. Amato, V. Piccialli, M. Varra, G. Piccialli, L. Mayol, *Tetrahedron* **2010**, *66*, 1931–1936; e) S. D’Errico, G. Oliviero, J. Amato, N. Borbone, V. Cerullo, A. Hemminki, V. Piccialli, S. Zaccaria, L. Mayol, G. Piccialli, *Chem. Commun.* **2012**, *48*, 9310–9312; f) V. Piccialli, S. D’Errico, N. Borbone, G. Oliviero, R. Centore, S. Zaccaria, *Eur. J. Org. Chem.* **2013**, 1781–1789.
- [8] H. Gehlen, G. Robish, *Justus Liebigs Ann. Chem.* **1962**, *660*, 148–154.
- [9] K. T. Potts, C. Hirsch, *J. Org. Chem.* **1968**, *33*, 143–150.
- [10] a) R. Faure, E. J. Vincent, J. Elguero, *Tetrahedron Lett.* **1973**, *29*, 2703–2706; b) R. M. Claramunt, J. P. Fayet, M. C. Vertut, P. Mauret, J. Elguero, *Tetrahedron* **1975**, *31*, 545–548.
- [11] A. K. Padhy, V. L. Nag, C. S. Panda, *Indian J. Chem. Sect. B* **1999**, *38*, 998–1001.
- [12] R. Centore, A. Carella, S. Fusco, *Struct. Chem.* **2011**, *22*, 1095–1103.
- [13] As a useful comparison we can mention that, in the case of biphenyl, the planar conformation has an energy 1.1 kcal/mol higher than that the twisted conformation (M. Akiyama, T. Watanabe, M. Kakihana, *J. Phys. Chem.* **1986**, *90*, 1752–1755). However, in our case, the steric hindrance for the 1,6 contact between the *ortho* hydrogens is considerably reduced because the internal angle of the five-membered ring is smaller than for the benzene ring (105° instead of 120°).
- [14] G. M. Sheldrick, *SADABS*, Bruker-Nonius, Delft, The Netherlands, **2002**.
- [15] A. Altomare, M. C. Burla, M. Camalli, G. L. Cascarano, C. Giacovazzo, A. Guagliardi, G. G. Moliterni, G. Polidori, R. Spagna, *J. Appl. Crystallogr.* **1999**, *32*, 115–119.
- [16] G. M. Sheldrick, *Acta Crystallogr., Sect. A* **2008**, *64*, 112–122.
- [17] L. J. Farrugia, *J. Appl. Crystallogr.* **1999**, *32*, 837–838.
- [18] C. F. Macrae, I. J. Bruno, J. A. Chisholm, P. R. Edgington, P. McCabe, E. Pidcock, L. Rodriguez-Monge, R. Taylor, J. van de Streek, P. A. Wood, *J. Appl. Crystallogr.* **2008**, *41*, 466–470.
- [19] J. Tomasi, B. Mennucci, R. Cammi, *Chem. Rev.* **2005**, *105*, 2999–3093.
- [20] M. J. Frisch, G. W. Trucks, H. B. Schlegel, G. E. Scuseria, M. A. Robb, J. R. Cheeseman, G. Scalmani, V. Barone, B. Mennucci, G. A. Petersson, H. Nakatsuji, M. Caricato, X. Li, H. P. Hratchian, A. F. Izmaylov, J. Bloino, G. Zheng, J. L. Sonnenberg, M. Hada, M. Ehara, K. Toyota, R. Fukuda, J. Hasegawa, M. Ishida, T. Nakajima, Y. Honda, O. Kitao, H. Nakai, T. Vreven, J. A. Montgomery, Jr, J. E. Peralta, F. Ogliaro, M. Bearpark, J. J. Heyd, E. Brothers, K. N. Kudin, V. N. Staroverov, R. Kobayashi, J. Normand, K. Raghavachari, A. Rendell, J. C. Burant, S. S. Iyengar, J. Tomasi, M. Cossi, N. Rega, J. M. Millam, M. Klene, J. E. Knox, J. B. Cross, V. Bakken, C. Adamo, J. Jaramillo, R. Gomperts, R. E. Stratmann, O. Yazyev, A. J. Austin, R. Cammi, C. Pomelli, J. W. Ochterski, R. L. Martin, K. Morokuma, V. G. Zakrzewski, G. A. Voth, P. Salvador, J. J. Dannenberg, S. Dapprich, A. D. Daniels, Ö. Farkas, J. B. Foresman, J. V. Ortiz, J. Cioslowski, D. J. Fox, *Gaussian 09*, rev. A.02, Gaussian, Inc., Wallingford, CT, **2009**.
- [21] *TURBOMOLE*, v. 6.3 (2011), a development of the University of Karlsruhe and Forschungszentrum Karlsruhe GmbH, *TURBOMOLE GmbH*, **1989–2007**; available from www.turbomole.com.
- [22] B. H. Besler, K. M. Merz Jr., P. A. Kollman, *J. Comput. Chem.* **1990**, *11*, 431–439.
- [23] A. Capobianco, A. Esposito, T. Caruso, F. Borbone, A. Carella, R. Centore, A. Peluso, *Eur. J. Org. Chem.* **2012**, 2980–2989.
- [24] A. Capobianco, R. Centore, C. Noce, A. Peluso, *Chem. Phys.* **2013**, *411*, 11–16.

Received: December 6, 2012

Published Online: ■